Bifunctional acoustic metamaterial lens designed with coordinate transformation

Citation: Zhu, Rongrong, et al. "Bifunctional Acoustic Metamaterial Lens Designed with Coordinate Transformation." Applied Physics Letters, vol. 110, no. 11, Mar. 2017, p. 113503. © 2017 Authors

As Published: http://dx.doi.org/10.1063/1.4978689

Publisher: AIP Publishing

Persistent URL: http://hdl.handle.net/1721.1/119152

Version: Final published version: final published article, as it appeared in a journal, conference proceedings, or other formally published context

Bifunctional acoustic metamaterial lens designed with coordinate transformation

Rongrong Zhu,[1,a)] Chu Ma,[2,a)] Bin Zheng,[1,b)] Muhyiddeen Yahya Musa,[1] Liqiao Jing,[1] Yihao Yang,[1] Huaping Wang,[3] Shahram Dehdashti,[1] Nicholas X. Fang,[2] and Hongsheng Chen[1,b)]

[1]*State Key Laboratory of Modern Optical Instrumentation, College of Information Science and Electronic Engineering, Zhejiang University, Hangzhou 310027, China*
[2]*Department of Mechanical Engineering, Massachusetts Institute of Technology, 77 Massachusetts Avenue, Cambridge, Massachusetts 02139-4307, USA*
[3]*Institute of Marine Electronics Engineering, Zhejiang University, Hangzhou 310027, China*

(Received 12 January 2017; accepted 3 March 2017; published online 16 March 2017)

We propose a method to design bifunctional acoustic lens using acoustic metamaterials that possess separate functions at different directions. The proposed bifunctional acoustic lens can be implemented in practice with subwavelength unit cells exhibiting effective anisotropic parameters. With this methodology, we experimentally demonstrate an acoustic Luneburg-fisheye lens at operational frequencies from 6300 Hz to 7300 Hz. Additionally, a bifunctional acoustic square lens is proposed with different focal lengths for multi directions. This method paves the way to manipulating acoustic energy flows with functional lenses. *Published by AIP Publishing.*
[http://dx.doi.org/10.1063/1.4978689]

Metamaterials are composite structures composed of periodic or quasiperiodic subwavelength unit cells, which have shown extraordinary wave properties beyond natural materials.[1–13] This concept was first suggested as optical devices to control the propagation of electromagnetic fields, and then extended to acoustics, due to the fact that the dynamical equations in both cases, i.e., electromagnetic[1–7] and acoustic waves,[8–12] have a similar relation with properties of the associated context environment. These similarities pave the way for exploiting the acoustic analog of interesting electromagnetics phenomena. The key to design both optic and acoustic metamaterials lies in the design of effective material properties.[14] Until now, acoustic metamaterials with extreme anisotropy,[8,9] negative mass density and bulk modulus,[15,16] enhanced absorption,[17,18] etc., have been designed. Synonymous with electromagnetic waves, novel devices can also be realized in acoustics like invisibility cloaks,[19–23] acoustic absorbers,[11] and gradient lenses.[12,24–27]

The refractive index of gradient index lenses (GRIN lenses) changes continuously in space following a specific function.[28] A number of GRIN lenses have been proposed theoretically to perform different imaging effects in geometrical optics such as Luneburg lens,[29] Maxwell-fisheye lens,[30] Eaton lens,[31] etc., which are widely used in optical information processing and communication applications.[32,33] Extending the design of optical devices into acoustics is an interesting scientific concept. The acoustic Luneburg lens, focusing the incoming acoustic wave on the edge of the opposite side of the lens, has been realized by aluminum columns arranged in a cylindrical shape.[34] However, the GRIN lenses designed previously can only work for a single function. A combination of two different functions in a single device will provide more flexibility in practice. Although a planar bifunctional Luneburg-fisheye lens made of anisotropic metasurface has been proposed in electromagnetics for surface waves,[35] a bifunctional lens that works for acoustic wave is still elusive.

In this paper, we propose a method to design the bifunctional acoustic lens which combines two different acoustic lens functions in a single device. The bifunctional effect is achieved by controlling the anisotropic refractive index distribution using structured acoustic metamaterials. Simulated and experimental results show that the designed lens can effectively achieve two different functions: Luneburg lens in the horizontal direction and fisheye lens in the vertical direction.

We first describe the principles of designing acoustic Luneburg-fisheye lens. Luneburg lens[29] is a kind of GRIN lens, as shown in Figure 1(a), which focuses the incoming plane wave to a point on the edge of the lens. It has a circularly symmetric refractive index distribution with the index of refraction n changing gradually according to the relation $n(r) = \sqrt{2 - (r/R)^2}$, where R is the radius of the circle and r is the radial distance from the center of the circle. A Maxwell's fisheye lens,[30] on the other hand, is a kind of GRIN lens that can focus the wave from a point source on the edge of the lens to another point on the opposite edge of the lens, shown in Figure 1(b). It also has a circularly symmetric refractive index distribution with the index of refraction n changing gradually according to another relation $n(r) = n_0/\left(1 + (r/R)^2\right)$, where n_0 is the maximum refraction index at the center of the lens, R is the radius of the circle, and r is the radial distance from the center of the circle. Owing to the inhomogeneous refractive index distributions of both lenses, it was extremely difficult to combine these two lenses together in one single device using natural materials. However, the problem can be solved by using acoustic metamaterials with anisotropic acoustic parameters.

[a)]R. Zhu and C. Ma contributed equally to this work.
[b)]Electronic addresses: zhengbin@zju.edu.cn and hansomchen@zju.edu.cn.

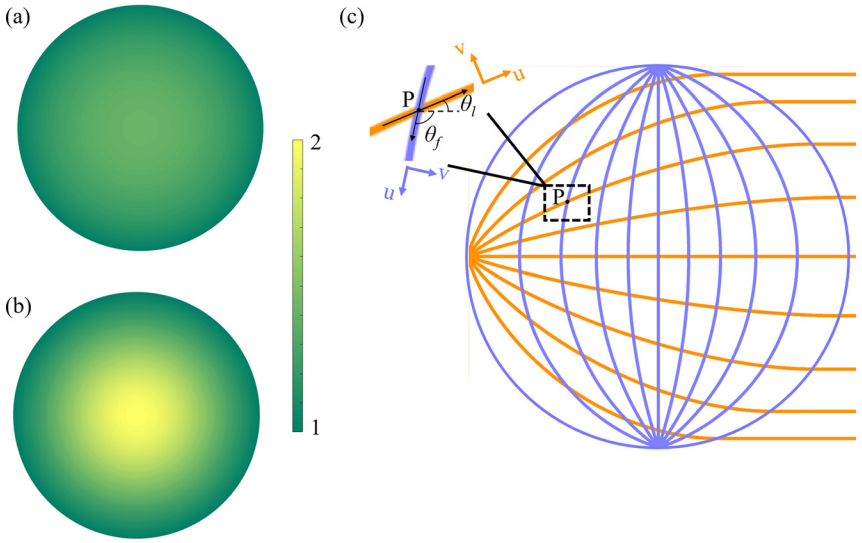

FIG. 1. (a) The refractive index distribution of Luneburg lens. (b) The refractive index distribution of fisheye lens. (c) The ray tracing of the bifunctional lens after combining the Luneburg and fisheye lenses together. θ_l and θ_f are the propagating angles at the same point for the Luneburg lens and the fisheye lens, respectively.

Figure 1(c) shows the ray approximation diagram of our proposed bifunctional acoustic lens. The lens behaves as a Luneburg lens in the horizontal direction for the point source located on the left side edge. As the ray propagates to point P, the direction of the ray changes to the angle of θ_l referring to the horizontal axis. Along the θ_l direction, the required effective refractive index of propagating wave is n_l, subjected to the refractive index equation of Luneburg lens at point P. Similarly, the lens behaves as a fisheye lens in the vertical direction for the point source located on the top side edge. As the ray propagates to the same point P, the direction of the ray changes to another angle θ_f away from the horizontal axis. To satisfy the ray trajectory in the lens, the required effective refractive index n_f along the ray direction θ_f should also satisfy the refractive index equation of fisheye lens at point P. Combining these two requirements together, the effective refractive index at point P should be anisotropic with n_l along the θ_l direction and n_f along the θ_f direction, simultaneously, instead of an isotropic refractive index.

Acoustic metamaterials with anisotropic densities can meet such a requirement. Suppose a metamaterial unit cell has relative density of ρ_x along the horizontal direction and ρ_y along the vertical direction, while the relative bulk modulus is B_0 and isotropic, the anisotropic refractive indices of such a unit cell will be $n_x = \sqrt{\rho_x/B_0}$ and $n_y = \sqrt{\rho_y/B_0}$. When the ray incidents onto this unit cell with an oblique angle θ with respect to the x axis, we can rotate the x-y axes counterclockwise by the same angle θ to form a new coordinate system, denoted by u-v axes. The rotation can be regarded as a coordinate transformation as follows:[36]

$$\begin{cases} u = x\cos\theta + y\sin\theta \\ v = y\cos\theta - x\sin\theta. \end{cases} \tag{1}$$

The refractive index tensor in this new coordinate system can be obtained,

$$\begin{cases} n_{uu} = n_x\cos^2\theta + n_y\sin^2\theta \\ n_{uv} = n_{vu} = (n_y - n_x)\cos\theta\sin\theta \\ n_{vv} = n_y\cos^2\theta + n_x\sin^2\theta. \end{cases} \tag{2}$$

For the point in our bifunctional lens where the ray is propagating with an oblique angle θ with respect to the x-axis, namely, along the u-axis, the effective refractive index of the ray will be n_{uu}. Since there are two different angles θ_l and θ_f at the same point, respectively, for the Luneburg lens and fisheye lens, the refractive indices of n_x and n_y should be chosen to make the effective refractive index n_{uu} approximately the same as the refractive index equations for the Luneburg lens n_l and fisheye lens n_f at the two different angles at that point, respectively, as shown in the following equation:

$$\begin{cases} n_x\cos^2\theta_l + n_y\sin^2\theta_l = n_l \\ n_x\cos^2\theta_f + n_y\sin^2\theta_f = n_f \end{cases}. \tag{3}$$

It should also be noted that, from Equation (2), there exists a cross-coupling factor n_{uv} between the u-v directions. This coupling term can be diminished by forcing n_x and n_y to be approximately identical.

Sequel to the design principles of anisotropic refractive indices, we propose a physical structure to verify the effect of our Luneburg-fisheye lens. The unit cell of the lens is shown in the inset of Figure 2(a), which is a cross-shaped structure made of a sound hard material placed in air. The periods of the unit cell are $l_1 = 5.7$ mm and $l_2 = 7.6$ mm, while the width of the cross line is $d_1 = 0.8$ mm. By changing the lengths a_1 and a_2, the anisotropic refractive indices can be controlled and have the ability to cover the parameter space calculated from Equation (3) at the working frequency around 6800 Hz. In Figure 2(a), we calculate the effective refractive indices from reflection and transmission coefficients[37] of two typical unit cells. It shows that this cross-shaped structure can effectively control the anisotropic effective refractive indices with a large tuning range. It should be noted that the cross-shaped structure is a resonant structure with the resonance frequency higher than the operating frequency in this paper. So all of the refractive index curves are dispersive. However, within the frequency range 4000 Hz–8000 Hz, the structure with larger a_1 and a_2 (with lower resonance frequency) has a stronger dispersion compared with the one in a smaller size (with higher resonance frequency). Figures 2(b) and 2(c)

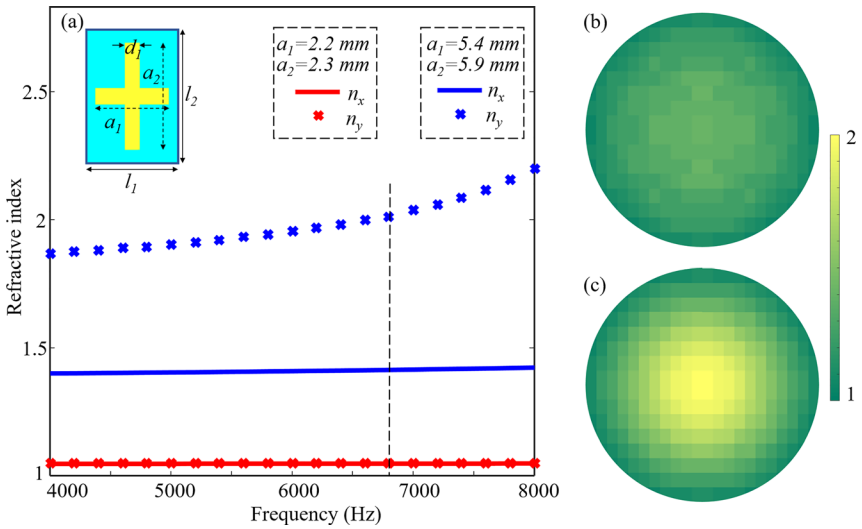

FIG. 2. (a) Dispersive refractive index of the cross-shaped structure. At the frequency of 6800 Hz, the effective properties of the unit cell are $n_x = 1.05$ and $n_y = 1.05$ for $a_1 = 2.2$ mm and $a_2 = 2.3$ mm, while $n_x = 1.41$ and $n_y = 2$ for $a_1 = 5.4$ mm and $a_2 = 5.9$ mm. (b) Distribution of n_x for the practical structure. (c) Distribution of n_y for the practical structure.

show the distribution of refractive indices for the unit cells of the experimental structure.

The 2D schematic diagram of our designed bifunctional Luneburg-fisheye lens, which is composed of 296 unit cells with 74 different dimensions, is shown in Figure 3(a). The designed lens is fabricated using DSM Somos® 14120 photopolymer by a 3D printing method. The polymer behaves as a sound hard material in air background. The cross-sections of unit cells in the fabricated prototype are in the same shapes as in Figure 3(a) with the height of each unit cell to be

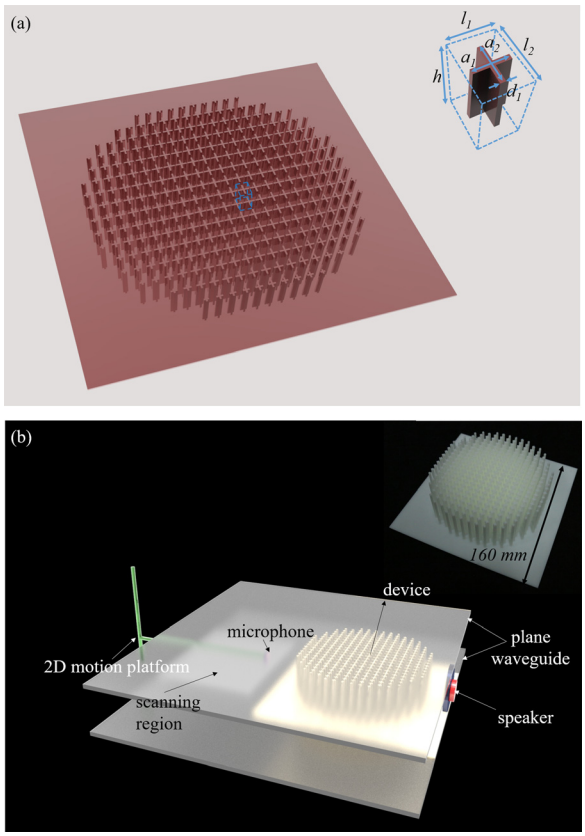

FIG. 3. (a) Schematic view of the bifunctional Luneburg-fisheye lens with the cross-shaped unit cell structure. The whole lens is composed of 296 unit cells with 74 different dimensions. (b) The experimental setup for the measurement. The top right inset is the prototype of the designed device.

40 mm. The measurement is performed in a plane waveguide and the experimental setup is shown in Figure 3(b), while the prototype of the designed device is also shown in the inset. The signal is generated by a speaker (which is approximate to a point source) at 10 mm away from the lens. The wave passes through the lens, gets scanned by a microphone and is then sent to an oscilloscope and a computer. The scanning region is a rectangle of the size 10 cm × 12.5 cm.

Figures 4(a) and 4(b) show the simulation results for two different incident directions at the frequency of 6800 Hz which are performed using finite element methods with COMSOL MULTIPHYSICS 5.0. The structure and the material parameters are the same as those mentioned in Figure 3. The point source is also placed 10 mm away from the lens and the incident pressure field excited by the point source located on the left is converted to the plane wave on the right through the device shown in Figure 4(a), while in Figure 4(b), the wave from point source located on top of the lens is converted to another point source on the bottom of the lens. We also verified the performance with the experiment. The measurement region is shown in the dashed box area in Figures 4(a) and 4(b), while Figures 4(c) and 4(d) show the measured acoustic pressure fields at the same frequency after the wave propagates through the designed lens in two different directions, respectively. The experimental results show good agreement with the simulated ones, validating that our designed acoustic metamaterials possesses the required anisotropic refractive indices and our bifunctional lens works well as predicted. To quantitatively illustrate the performance of our lens, experimental data of normalized pressure amplification along the line from $x = 90$ mm to $x = 190$ mm at $y = 0$ mm for the point source excited on the left and the line from $y = 90$ mm to $y = 190$ mm at $x = 0$ mm for the point source excited on the top are shown in Figure 4(e). At a frequency of 6300 Hz, 6800 Hz, and 7300 Hz, the measured pressure field maintains as a plane wave for a point source located on the left while scatter as a point source for a point source located on the top, which also demonstrates the broad frequency band of our device.

Additionally, by utilizing the same method, we also propose a bifunctional square lens which has different focal lengths

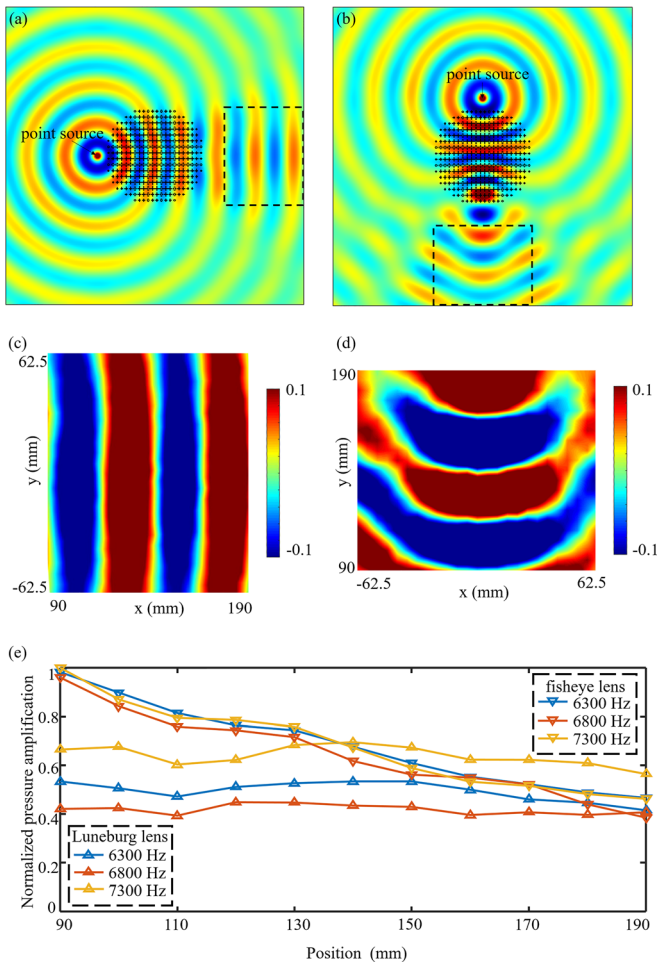

FIG. 4. Simulation results (a) and (b) and experimental results (c) and (d) of the bifunctional Luneburg-fisheye lens. The point source is 10 mm away from the lens at 6800 Hz. (a) Pressure field of a point source put in the left, the lens behave like a Luneburg lens. (b) Pressure field of a point source put in the top, the lens behave like a fisheye lens. (c) Measured acoustic pressure field of the region in (a). (d) Measured acoustic pressure field of the region in (b). (e) Experimental data of normalized pressure amplification at $y = 0$ mm of (c) which act as Luneburg lens and $x = 0$ mm of (d) that act as fisheye lens at the frequency of 6300 Hz, 6800 Hz, and 7300 Hz.

for different incident directions. As shown in Figures 5(a) and 5(b), the refractive indices of the square GRIN focal lens are changing along the direction transverse to incident axis, which enables redirection of incident wave trajectories inside the lens. In Figure 5(a), the refractive index profile of the square GRIN focal lens[18] is $n(y) = n_0\mathrm{sech}(\alpha y)$, which gives a focal length of $f = \pi/2\alpha$ for rays incident from the left. Here, n_0 is the refractive index along the x-axis and α is the gradient coefficient. Similarly, as shown in Figure 5(b), rays incident from the top into a square GRIN focal lens will have the refractive index profile in the form of $n(x) = n_0\mathrm{sech}(\alpha x)$. By varying the gradient coefficients, the focal length of the GRIN lens can be adjusted. In Figures 5(a) and 5(b), we choose the focal lengths in the two directions to be $f = l/2$ and $f = l$, respectively, where l is the side length of the square GRIN lens. With the same method used for designing the Luneburg-fisheye lens, we can combine these two square lenses using anisotropic acoustic metamaterials. Figure 5(c) shows the schematic diagram of the bifunctional square lens. It is composed of 432 unit cells with 108 different shapes. The unit cell is an H-shaped sound hard structure at the center of the air background. The period of the unit cell is the same as that for the previous circular lens in Figure 3 and the width of the H-shaped line is $d_2 = 0.4$ mm. By adjusting the lengths b_1 and b_2, we can also control the anisotropic parameters to satisfy the required refractive index tensor for the bifunctional square lens.

Simulation is also performed at the working frequency of 6800 Hz to verify the performance of the designed bifunctional square lens and the results are shown in Figure 6. In Figure 6(a), a plane wave is incident from the line source on the left of the device. The acoustic wave focuses at the center of the lens and diverges out of the lens as a plane wave again as predicted in Figure 5(a). On the other hand, when the line source is at the top of the device, the acoustic wave propagates in the device and focuses at the bottom side of the square lens, as predicted in Figure 5(b). The results show that this bifunctional square lens can also work effectively as designed.

We have combined a Luneburg lens and a fisheye lens into a single device using non-uniform anisotropic acoustic metamaterials. A bifunctional acoustic Luneburg-fisheye lens is designed and experimentally verified. A bifunctional square lens is also designed and the simulation results show good agreement as predicted. Our design method can be used to combine many other lens types to design different bifunctional lenses in acoustics.

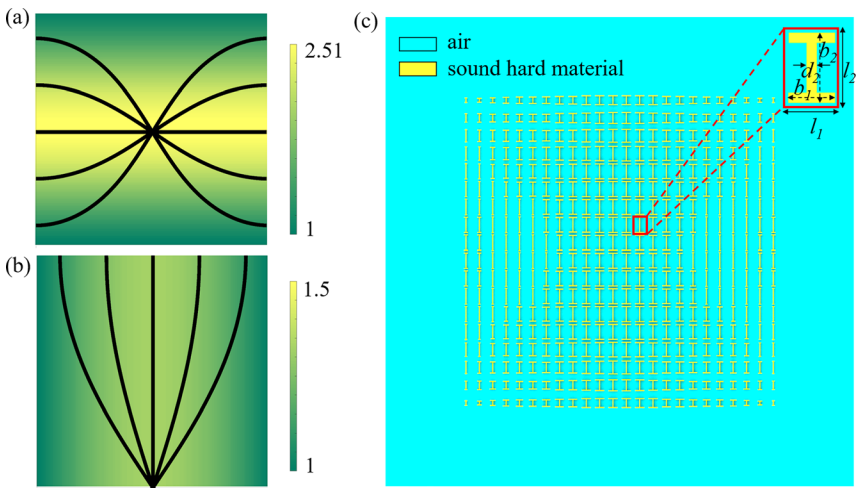

FIG. 5. (a) The refractive index distribution and the ray tracing of the square lens. Rays incident from left to right and the focus point is at the center of the lens. (b) The refractive index distribution and the ray tracing of the square lens. Rays incident from top to bottom and the focus point is at the edge of the lens. (c) Schematic view of the bifunctional square lens with the H-shaped unit cell structures. The whole lens is composed of 432 unit cells with 108 different dimensions.

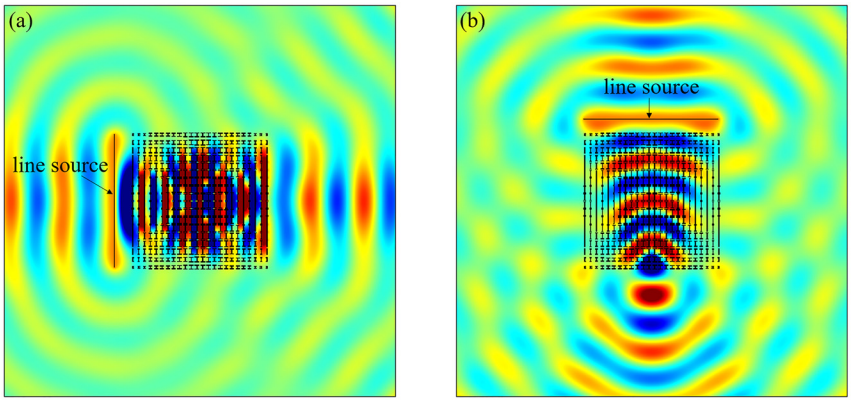

FIG. 6. Simulation results of the bifunctional square lens. The line source is at 15 mm away from the lens. (a) Pressure field of the line source put in the left, the plane wave focuses in the middle of the lens and diverges to be a plane wave on the right side of the lens. (b) Pressure field of line source put in the top, the plane wave focuses in the edge of the lens and behaves like a point source from the bottom side of the lens.

This work was sponsored by the National Natural Science Foundation of China under Grant Nos. 61625502, 61574127, and 61601408; the ZJNSF under Grant No. LY17F010008; the Postdoctoral Science Foundation of China under Grant No. 2015M581930; the Top-Notch Young Talents Program of China; and the Innovation Joint Research Center for Cyber-Physical-Society System. Nicholas Fang and Chu Ma acknowledge the financial support from the MIT Sea Grant College Program, under NOAA Grant No. NA10OAR4170086, MIT SG Project No. 2015-R/RCM-41.

[1]C. Caloz and T. Itoh, *Electromagnetic Metamaterials: Transmission Line Theory and Microwave Applications* (John Wiley & Sons, 2005).
[2]X. Zhang and Z. Liu, Nat. Mater. **7**, 435 (2008).
[3]J. A. Dockrey, M. J. Lockyear, S. J. Berry, S. A. R. Horsley, J. R. Sambles, and A. P. Hibbins, Phys. Rev. B **87**, 125137 (2013).
[4]J. B. Pendry, D. Schurig, and D. R. Smith, Science **312**, 1780 (2006).
[5]Z. Wang, F. Cheng, T. Winsor, and Y. Liu, Nanotechnology **27**, 412001 (2016).
[6]N. Engheta and R. W. Ziolkowski, *Metamaterials: Physics and Engineering Explorations* (John Wiley & Sons, 2006).
[7]H. Wang, Y. Deng, B. Zheng, R. Li, Y. Jiang, S. Dehdashti, Z. Xu, and H. Chen, Sci. Rep. **7**, 40083 (2017).
[8]J. Christensen and F. J. G. de Abajo, Phys. Rev. Lett. **108**, 124301 (2012).
[9]C. Shen, J. Xu, N. X. Fang, and Y. Jing, Phys. Rev. X **4**, 041033 (2014).
[10]S. H. Lee, C. M. Park, Y. M. Seo, Z. G. Wang, and C. K. Kim, J. Phys.-Condens. Mater. **21**, 175704 (2009).
[11]R. Q. Li, X. F. Zhu, B. Liang, Y. Li, X. Y. Zou, and J. C. Cheng, Appl. Phys. Lett. **99**, 193507 (2011).
[12]T. P. Martin, M. Nicholas, G. J. Orris, L. W. Cai, D. Torrent, and J. Sánchez-Dehesa, Appl. Phys. Lett. **97**, 113503 (2010).
[13]F. Gao, Z. Gao, X. Shi, Z. Yang, X. Lin, H. Xu, J. D. Joannopoulos, M. Soljačić, H. Chen, L. Lu, Y. Chong, and B. Zhang, Nat. Commun. **7**, 11619 (2016).
[14]M. Schoenberg and P. N. Sen, J. Acoust. Soc. Am. **73**, 61 (1983).
[15]J. Li and C. T. Chan, Phys. Rev. E **70**, 055602 (2004).
[16]Y. Ding, Z. Liu, C. Qiu, and J. Shi, Phys. Rev. Lett. **99**, 093904 (2007).
[17]A. Climente, D. Torrent, and J. Sánchez-Dehesa, Appl. Phys. Lett. **100**, 144103 (2012).
[18]J. Mei, G. Ma, M. Yang, Z. Yang, W. Wen, and P. Sheng, Nat. Commun. **3**, 756 (2012).
[19]B. I. Popa and S. A. Cummer, Phys. Rev. B **83**, 224304 (2011).
[20]J. B. Pendry and J. Li, New J. Phys. **10**, 115032 (2008).
[21]B. I. Popa, L. Zigoneanu, and S. A. Cummer, Phys. Rev. Lett. **106**, 253901 (2011).
[22]Y. Yang, H. Wang, F. Yu, Z. Xu, and H. Chen, Sci. Rep. **6**, 20219 (2016).
[23]R. Zhu, B. Zheng, C. Ma, J. Xu, N. Fang, and H. Chen, J. Acoust. Soc. Am. **140**, 95 (2016).
[24]A. Climente, D. Torrent, and J. Sánchez-Dehesa, Appl. Phys. Lett. **97**, 104103 (2010).
[25]L. Zigoneanu, B. I. Popa, and S. A. Cummer, Phys. Rev. B **84**, 024305 (2011).
[26]S. C. S. Lin, T. J. Huang, J. H. Sun, and T. T. Wu, Phys. Rev. B **79**, 094302 (2009).
[27]T. M. Chang, G. Dupont, S. Enoch, and S. Guenneau, New J. Phys. **14**, 035011 (2012).
[28]J. C. Garnett and J. G. Valentine, *CLEO: Applications and Technology* (Optical Society of America, 2012), Vol. 88.
[29]A. S. Gutman, "Modified Luneburg lens," J. Appl. Phys. **25**, 855 (1954).
[30]B. Fuchs, O. Lafond, S. Rondineau, and M. Himdi, IEEE Trans. Microwave Theory **54**, 2292 (2006).
[31]T. Zentgraf, Y. Liu, M. H. Mikkelsen, J. Valentine, and X. Zhang, Nat. Nanotechnol. **6**, 151 (2011).
[32]S. Dehdashti, R. Li, X. Liu, M. Raoofi, and H. Chen, Laser Phys. **25**, 075201 (2015).
[33]H. M. Moya-Cessa, F. Soto-Eguibar, V. Arrizon, and A. Zuniga-Segunbo, Opt. Express **24**, 10445 (2016).
[34]S.-H. Kim, in *2014 8th International Congress on Advanced Electromagnetic Materials in Microwaves and Optics (METAMATERIALS)* (IEEE, 2014).
[35]X. Wan, X. Shen, Y. Luo, and T. J. Cui, Laser Photonics Rev. **8**, 757 (2014).
[36]S. Xi, H. Chen, B. I. Wu, and J. A. Kong, IEEE Microwave Wireless Compon. **19**, 131 (2009).
[37]V. Fokin, M. Ambati, C. Sun, and X. Zhang, Phys. Rev. B **76**, 144302 (2007).